Álvarez Polegre, A., Pérez Leal, R., García García, J. A. & García Armada, A. (18-21 June 2019). *Drive tests-based evaluation of macroscopic pathloss models for mobile networks* [proceedings]. European Conference on Networks and Communications (EuCNC-2019), Valencia, Spain.

DOI: 10.1109/EuCNC.2019.8802061

Drive Tests-based Evaluation of Macroscopic Pathloss Models for Mobile Networks

Alberto Álvarez Polegre*, Raquel Pérez Leal*, José Antonio García García†, Ana García Armada*
aalvarez@tsc.uc3m.es, rpleal@tsc.uc3m.es, jose-antonio.garcia@nokia.com, agarcia@tsc.uc3m.es
*Deparment of Signal Theory and Communications, University Carlos III de Madrid
†Nokia Spain

***Abstract*—Mobile operators have already started their 5G network deployment and next generation user terminals commercial release is planned for the upcoming months. Knowing the future network system performance and capabilities seem to be key in order to have proper planning strategies. In this paper we present some field test trials for the latest release of 4G, which have lots of similarities with the forthcoming mobile broadband standard. Results for urban drive tests are presented too. We also bring pathloss simulation based on modern channel models that matches the results obtained in the real scenarios. Error is measured to have insights about the utility and accuracy of the pathloss models when comparison with specific scenarios is made. Some final brainstorming for future work with 5G network and concluding remarks are proposed.**

***Index Terms*—Drive tests, field test, pathloss, RSSI, LTE-A.**

I. Introduction

The 3rd Generation Partnership Project (3GPP) has recently approved the standalone version of the next mobile broadband communications standard, named fifth generation New Radio (5G NR) [1], back in July 2018 [2]. This fact, along with the availability of recently developed 5G chipsets for user terminals is paving the way for mobile communications operators to start deploying the first 5G radio equipment and perform the first 5G NR field test trials. These test trials aim to evaluate the radio performance at a system level in a close-to-real environment [3], in spite of previous testing focused on specific radio aspects carried out on test beds presented in the scientific literature, such as [4] and [5], which are intended to test waveform performance and multi-antenna behavior, respectively.

The first commercial release of 5G user terminals is planned for 2019 and network deployment may start in 2019-2020. However, the evolution of the mobile networks towards 5G from 4G will follow a stepwise approach with different architecture options and migration from the Long Term Evolution (LTE) standard. That leads to a set of transition scenarios. From initial scenarios based on the incumbent enhanced LTE networks, i.e. LTE-Advanced (LTE-A) and LTE-Advanced Pro (LTE-A Pro) systems, that will consist on enhanced radio access network (RAN) and enhanced packet core (EPC), to fully IMT-2020 compliant 5G networks [6], [7], [8], that will include the next generation core (NGC) and new radio of the future 5G networks [9].

Apart form the measurement campaigns, new models and simulation tools are required to verify and to improve performance, i.e. user throughput, interference management, resource allocation, etc., in next generation scenarios, and to predict, more efficiently, the behavior when migrating to 5G NR technologies. In order to move on in this direction, in this paper field tests at fixed locations and drive tests based on the latest release of LTE-A Pro are made. Simulations with proper adjustments are done to cope with the measured parameters as much as possible. Simulations are partly based on the Vienna Cellular Communications Simulators (VCCS) LTE-A Downlink System Level Simulator [10]. The matching between the simulation and measured results obtained are fairly good in most cases. This testing is intended to provide a basic understanding that can be extrapolated for 5G NR scenarios so we have an accurate prediction of its performance for the very early releases.

The reminder of this paper is organized as follows. Section II details the measurements campaign and its data recording procedure. Section III is devoted to the selection of a proper pathloss model and presentation of its formulation. Simulation results and comparison is presented in Section IV. Some concluding remarks are presented in Section V.

II. Measurements Campaign

We have carried out field test trials and drive tests in a medium size European city[1] which represents fairly well data traffic and both line-of-sight (LOS) and non-line-of-sight (NLOS) conditions. For every test we are using an LTE Cat.16 Samsung Galaxy S8 as user terminal (UE) which is capable of 4x4 MIMO communications. This UE is equipped with Nemo Handy Handheld Measurement Solution for recording all LTE parameters needed. Then, results log can be analyzed with a computer-based testing tool, Nemo Outdoor Drive Test Solution.

Among all the parameters that the software analyzer provides, we present here those we considerer are key when evaluating signal quality in a LTE-A transmission.

- Received Signal Strength Indicator (RSSI): Wideband received power from serving and non-serving cells at UE.
- Reference Signal Received Power (RSRP): Average power from resource elements (RE) carrying cell-specific reference signals.
- Reference Signal Received Quality (RSRQ): Ratio defined as $N\frac{RSRP}{RSSI}$, where N is the number of physical resource blocks (PRB).
- Channel Quality Indicator (CQI): Index between 1 and 15 reporting about channel quality conditions so the serving cell can choose a proper modulation and coding rate.

[1]Due to confidentiality reasons we cannot specify the place in which tests have taken place.

TABLE I
FREQUENCY BANDS AND CHANNEL BANDWIDTHS

LTE Band	Channel Bandwidth
L800	10 MHz
L2100	15 MHz
L1800	20 MHz
L2600	20 MHz

In order to have trusted results to compare with simulations, we have done first testing in fixed locations with well-known conditions, in words, locations where we can easily predict LOS and NLOS conditions as well as distance from the user to the corresponding serving and interfering cells. This let us choose and adjust the pathloss model properly for drive testing.

Thanks to the information provided by the corresponding network operator, we know the available LTE frequency bands and their channel bandwidth, as shown in Table I. We are also provided with the physical cell identity (PCI), which identifies a specific cell and sector and the evolved universal terrestrial radio access (EUTRA) absolute radio frequency channel number (EARFCN), which uniquely identifies the LTE band and carrier frequency regardless the channel bandwidth, apart from the exact location of every eNB and its height. Nemo Handy provides as well with the PCI and EARFCN. If the information displayed by Nemo Handy matches with the information provided by the operator, we can perfectly know which cell and sector the UE is connected to. Many other parameters are provided by Nemo Handy, though they are irrelevant in this work. In order to force the UE to generate downlink traffic, a very simple script loaded with Nemo Handy makes the eNB to send data to the terminal. The script sends this command through an infinite loop until the user stops it. This way we can test the transmission for as long as needed.

A. Field Tests

Six different locations have been chosen for initial testing with the intention of representing as much situations as possible that a mean UE may experience. As stated before, with the information of both the operator and Nemo Handy we undoubtedly know which cell and sector the UE is communicating with. Table II shows all the measured parameters for every location and LTE band, as well as distance to serving cell (d_s) and UE and eNB heights (h_{UE} and h_s, respectively). Distance to interfering cell (d_i) and interfering eNB height (h_i) are specified when applies. For indoor scenarios, d_s is split in outdoor section (d_s^{out}) and indoor section (d_s^{in}). The first three locations are situated at the city outskirts where only two eNB are available.

For the first location we have an outdoor LOS suburban scenario with UE being close to the serving eNB. Though there is a nearby interfering cell, it is not near enough to affect negatively to any of the measured parameters. The aim of the first test is to have fairly good channel conditions.

In the second location we reproduce the previous scenario getting closer to the other eNB in the surroundings. Thanks to the PCI we know that the UE attaches itself to it. It worth noting that, even though the interfering cell is closer

Fig. 1. Fixed locations 1, 2 and 3 and surrounding eNBs.

to the UE than the serving cell, the terrain between them is not completely flat. This may result in a higher pathloss and may be the reason why UE finds better channel quality with the eNB that is further away, instead of the closer one. Now interference and longer distance are key to evaluate the measuring parameters. Comparing with the previous situation, UE reports higher data rates. The serving cell is located at a pretty much isolated environment where a lower number of users is expected. This results in more PRBs assigned to every user and thus, higher throughput as measuring outputs state.

The third location shows very similar results as the second one, something expected knowing that conditions and distances between the UE and both eNBs are alike. Note that measurements for location 2 and 3 are made from inside a car, so additional losses need to be considered. We still consider both scenarios as outdoor, nevertheless. A map for these three locations is shown in Figure 1.

The next three locations take place within the city downtown. We have carried out one outdoor testing and two indoors. In location 4 the UE is situated in the second-floor of a building near the wall. This situation supposes an outdoor-to-indoor (O2I) NLOS scenario. Location 5 is a typical urban NLOS scenario where building mean height and streets mean width should be considered. Lastly, location 6 is similar to location 4, but UE is situated in the first-floor and deeper into the building. All these three scenarios results in pretty similar outputs in terms of data rate. Communication is not limited by signal strength but by the number of users and resources available to allocate to each one of them instead. Interference is not a limiting factor either, because UE is isolated from it, mostly in the indoor scenarios. The outdoor NLOS is the most common scenario that we will face when performing drive tests.

B. Drive Tests

For the drive testing we are using the same terminal as before, but this time it only operates at the L1800 LTE band. It is placed inside a public transport bus that travels around the streets of the city. Its route is shown in Figure 2. The looping script keeps on running until the end of the route. Nemo Handy generates data reporting about the measuring parameters every few milliseconds and thus, the size of the log file is considerably large. For the sake of drive test

TABLE II
FIELD TEST MEASURAMENTS

	LTE Band	RSSI	RSRP	RSRQ	CQI	Throughput
Fixed location 1	L800	-29 dBm	-58 dBm	-11 dB	10	76 Mbps
(outdoor)	L2100	-36 dBm	-70 dBm	-16 dB	10	87 Mbps
$d_s = 83\ m$	L1800	-32 dBm	-68 dBm	-15 dB	13	92 Mbps
$h_s = 15\ m,\ h_{UE} = 1.5\ m$	L2600	-36 dBm	-73 dBm	-14 dB	10	93 Mbps
Fixed location 2	L800	-52 dBm	-84 dBm	-13 dB	8	99 Mbps
(outdoor)	L2100	-59 dBm	-91 dBm	-10 dB	6	125 Mbps
$d_s = 550\ m,\ d_i = 410\ m$	L1800	-57 dBm	-92 dBm	-11 dB	8	120 Mbps
$h_s = 5\ m,\ h_i = 15\ m,\ h_{UE} = 1\ m$	L2600*	-	-	-	-	-
Fixed location 3	L800	-48 dBm	-76 dBm	-11 dB	8	98 Mbps
(outdoor)	L2100	-57 dBm	-88 dBm	-10 dB	10	115 Mbps
$d_s = d_i = 360\ m$	L1800	-68 dBm	-102 dBm	-13 dB	8	120 Mbps
$h_s = 5\ m,\ h_i = 15\ m,\ h_{UE} = 1\ m$	L2600*	-	-	-	-	-
Fixed location 4	L800	-45 dBm	-76 dBm	-12 dB	9	93 Mbps
(indoor)	L2100	-54 dBm	-88 dBm	-16 dB	8	105 Mbps
$d_s^{in} = 80\ m,\ d_s^{out} = 2\ m$	L1800	-47 dBm	-81 dBm	-14 dB	12	104 Mbps
$h_s = 35\ m,\ h_{UE} = 6\ m$	L2600	-50 dBm	-87 dBm	-16 dB	8	108 Mbps
Fixed location 5	L800	-45 dBm	-74 dBm	-11 dB	13	92 Mbps
(outdoor)	L2100	-43 dBm	-77 dBm	-15 dB	11	104 Mbps
$d_s = 70\ m$	L1800	-42 dBm	-77 dBm	-14 dB	11	106 Mbps
$h_s = 35\ m,\ h_{UE} = 2\ m$	L2600	-44 dBm	-78 dBm	-13 dB	12	111 Mbps
Fixed location 6	L800	-54 dBm	-82 dBm	-11 dB	9	100 Mbps
(indoor)	L2100	-60 dBm	-94 dBm	-15 dB	13	116 Mbps
$d_s^{in} = 80\ m,\ d_s^{out} = 7\ m$	L1800	-55 dBm	-89 dBm	-14 dB	13	117 Mbps
$h_s = 35\ m,\ h_{UE} = 2\ m$	L2600	-59 dBm	-95 dBm	-14 dB	7	126 Mbps

*Serving cell is not capable of transmitting at the L2600 band.

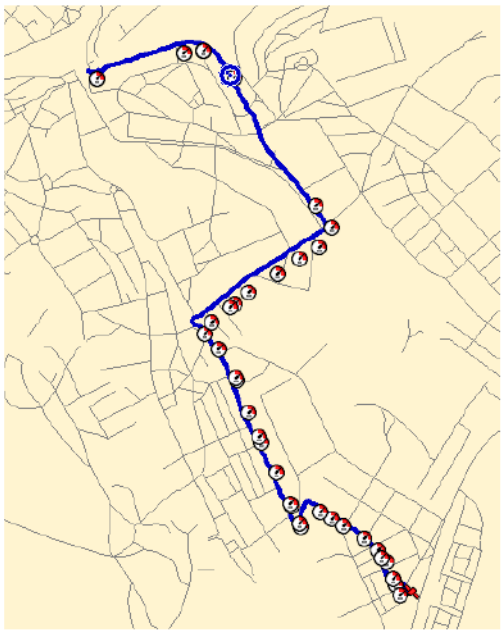

Fig. 2. Bus route used for drive tests displayed with Nemo Outdoor.

evaluation, only eight positions, i.e. eight time instants, are taken into consideration. Since we are aware of the location of every cell that the UE may connect to and its corresponding PCI, we can monitor the handover operation easily and know the distance to the serving and interfering eNBs. Measured parameters are shown in Table III with same notation as for the fixed position tests.

III. PATHLOSS MODEL

Once all the real environment measuring data is gathered, we need to choose a proper channel model that includes a pathloss modeling that matches as close as possible the measurements campaign results. The main parameter we analyzed is the RSSI level, defined as

$$RSSI = 10\log_{10}(P_s^r + \sum_{i=1}^{N_i} P_i^r) + G_{UE} \quad (1)$$

where N_i is the total number of interfering cells, P_s^r is the received power from serving cell and P_i^r is the received power from i-th interfering cell, both in linear units, and G_{UE} is the UE antenna gain in dBi. We define P_s^r as

$$P_s^r = 10^{\frac{P_s^t + G_s \quad L_t \quad L}{10}} \quad (2)$$

where P_s^t is the eNB transmission power in dBm, G_s is the eNB antenna gain in dBi, L_t is the insertion loss and L is the pathloss. Except for L, all these parameters are given by the operator. Note that for a same eNB P_s^t may be different depending on the LTE band used. L needs to be calculated using a pathloss model that suits our needs and behaves close to reality for the scenarios under evaluation.

There are several channel models with their corresponding pathloss mathematical formulation for mobile networks such as Okumura-Hata model [11] or ITU-R P.1411 [12] which is based on the COST231 model. However, these models have some restrictions regarding distance and frequency range and are not fully intended for LTE, but for general wireless communications instead. We find that the pathloss model included in the 3GPP technical report regarding LTE 3D channel model [13] suits much better for every situation and location we intend to reproduce. It addition, this channel

TABLE III
DRIVE TEST MEASUREMENTS

	RSSI	RSRP	RSRQ	CQI	Throughput
Bus position 1 $d_s = 280\ m,\ d_{i_1} = 500\ m,\ d_{i_2} = 236\ m$ $h_s = 7\ m,\ h_{i_1} = 35\ m,\ h_{i_2} = 21\ m$	-60 dBm	-93 dBm	-12 dB	7	112 Mbps
Bus position 2 $d_s = 100\ m,\ d_i = 550\ m$ $h_s = 7\ m,\ h_i = 35\ m$	-58 dBm	-93 dBm	-15 dB	6	115 Mbps
Bus position 3 $d_s = 300\ m,\ d_i = 340\ m$ $h_s = 7\ m,\ h_i = 35\ m$	-62 dBm	-95 dBm	-12 dB	9	115 Mbps
Bus position 4 $d_s = 230\ m$ $h_s = 35\ m$	-54 dBm	-84 dBm	-7 dB	12	102 Mbps
Bus position 5 $d_s = 230\ m$ $h_s = 35\ m$	-47 dBm	-84 dBm	-15 dB	9	104 Mbps
Bus position 6 $d_s = 500\ m,\ d_i = 212\ m$ $h_s = 35\ m,\ h_i = 18\ m$	-50 dBm	-83 dBm	-12 dB	9	98 Mbps
Bus position 7 $d_s = 700\ m,\ d_i = 274\ m$ $h_s = 35\ m,\ h_i = 18\ m$	-56 dBm	-91 dBm	-12 dB	8	110 Mbps
Bus position 6 $d_s = 480\ m$ $h_s = 18\ m$	-74 dBm	-106 dBm	-11 dB	11	125 Mbps

model is recommended by ITU-R [14] and serves as a basis in the 5G 3GPP channel model [15]. The pathloss formulation in this channel model includes calculation guidance for macro and micros cell environments, LOS and NLOS situation and O2I scenarios. Apart from the pathloss calculation itself, in some scenarios we need to consider additional penetration losses owing to the fact of being inside a car while measuring or terrain orography, among other considerations. For every simulation, the proper pathloss equation that this channel model provides is used ($L \triangleq PL$). For all formulation distance, height and street width are given in m and frequency is given in GHz. For the LOS scenarios the pathloss is defined as

$$PL_{LOS} = 22\log_{10}(d_{3D}) + 28 + 20\log_{10}(f_c) \tag{3}$$

where f_c is the carrier frequency and d_{3D} is the 3D distance between the eNB and the UE defined as

$$d_{3D} = \sqrt{d_{2D}^2 + (h_{eNB} - h_{UE})^2} \tag{4}$$

being d_{2D} the linear distance between the eNB and the UE and h_{eNB} the eNB height.

Now in the NLOS scenario, the pathloss is defined as

$$\begin{aligned} PL_{NLOS} = {} & 161.04 - 7.1\log_{10}(W) + 7.5\log_{10}(h) \\ & -\left(24.37 - 3.7\left(\frac{h}{h_{eNB}}\right)^2\right)\log_{10}(h_{eNB}) \\ & +(43.42 - 3.1\log_{10}(h_{eNB}))(\log_{10}(d_{3D}) - 3) \\ & +20\log_{10}(f_c) - (3.2(\log_{10}(17.625))^2 - 4.97) \\ & -0.6(h_{UE} - 1.5) \end{aligned} \tag{5}$$

where W is the streets mean width and h is the building mean height.

Finally, for the O2I scenario we have

$$PL_{O2I} = PL_{LOS}\big|_{d_{3D}^{in} + d_{3D}^{out}} + 20 + 0.5 d_{2D}^{in}. \tag{6}$$

IV. RESULTS EVALUATION

To rate our simulations, we measure the error between the measured RSSI and the simulated value defining this metric as

$$\Delta = |RSSI_{measured} - RSSI_{simulated}|. \tag{7}$$

Figure 3 shows the error for the field tests in every location and LTE band. We consider an error of 3-4 dB to be acceptable enough, since we are trying to replicate very concrete situation with a generic pathloss model. Note as well that this pathloss model is most accurate when the carrier frequency is between 2-6 GHz, so the error at the L800 band is expected to be high. In most locations the model is accurate enough except for the L1800 band in location 3 and for the L800 in most of the locations. Some measurements were discarded for the due to the impossibility of achieving good results through simulations. These few measurements were made in different types of terrain where the porosity of the terrain is not a variable that the pathloss model can predict.

Figure 4 shows same information, but for the drive tests. In this case we have a quasi-permanent NLOS outdoor situation with a changing environment in terms of building heights and obstacles. Error is much higher this time since we have less information to adjust the pathloss model. Even though these tests are run in a city where most buildings are the same height, it is not possible to simulate every concrete situation that the real pathloss experienced. Trees, traffic jams, spots without buildings, etc., are variables that a general pathloss model cannot predict or simulate with parameters. Nota that base station heights are not constant and vary from one to another. Due to the low speed of the bus, the doppler shift is not considered since it has little to no impact.

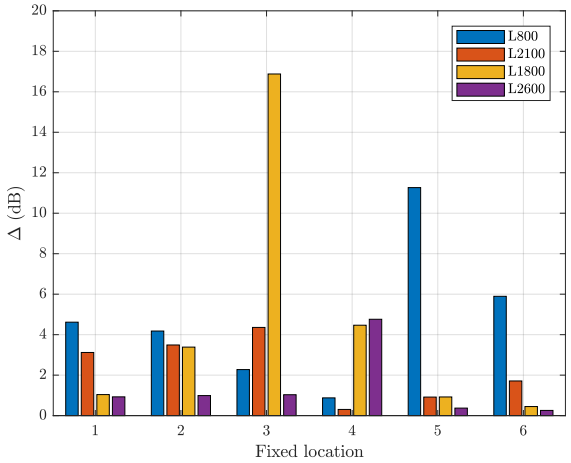

Fig. 3. Error measured for the field tests.

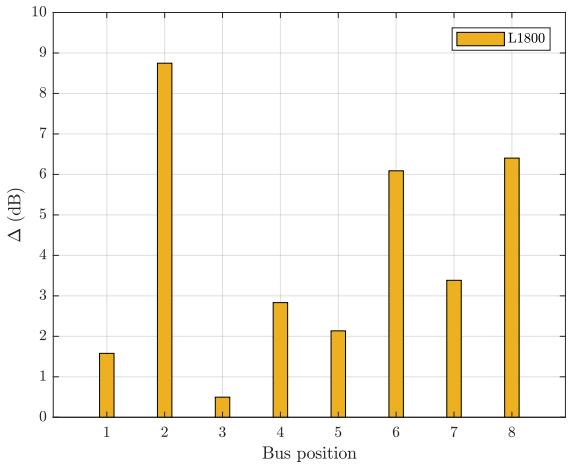

Fig. 4. Error measured for the drive tests.

V. Concluding Remarks

In this paper with have presented real LTE-A Pro measurements in a mean size city. Both fixed location testing for different environments and drive tests have been carried out. The most important parameters for rating the link quality and communication performance provided by a professional drive test software have been presented. With a proper pathloss model selection, we have simulated the RSSI level and measured the error with the real value. Except for certain situations, the model matches reality fairly well in known scenarios. Less accurate results are obtained for the drive test situation. It is clearly visible that no matter how accurate the pathloss model tends to be in theory, field test trials are key for evaluating the system performance. When draw upon drive tests, several measuring points should be analyzed so this way the pathloss mean error may tend to 0, if the model is accurate enough. As part of future work, CQI and throughput validation should be done. Knowing the transmission power and antenna gain from every eNB and their corresponding pathloss, one can estimate the SINR level at receiver and map it to the CQI value [16]. Throughput can be calculated using Shannon channel capacity formula, though it would most probably lead to very inaccurate values. In the LTE family standards, resource allocation and PRBs assignment are made through a scheduler that has a considerable impact on the effective user throughput. Plus, some operators and manufactures are already using machine learning techniques for resource allocation, a situation that would harden even more the throughput estimation. Mean number of users during the measurement campaign would be also needed.

Lastly, simulation scenarios should be modified to evaluate the results obtained using 5G NR. Higher order of multiple-input multiple-output (MIMO) communications, different carrier frequency, higher channel bandwidth for assigning more PRBs to UE or even wider subcarrier spacing could give some insights about the performance of 5G NR in the tested scenarios.

Acknowledgements

This work has been partly supported by the project OPALL5G: Optimization of Small Cells Performance in 5G NR of the Spanish CDTI PID Project and by the Spanish National Projects TERESA-ADA (TEC2017-90093-C3-2-R) (MINECO/AEI/FEDER, UE).

References

[1] *3GPP 5G New Radio Release 15*. Accessed on 20th February 2019. [Online]. Available: https://www.3gpp.org/release-15

[2] *5G NR Physical Layer General Description*, ETSI Std. TS 38.201 version 15.0.0 Release 15, 2018.

[3] Global Mobile Suppliers Associations, "Global Progress to 5G - Trials, Deployments and Launches," GSA, Tech. Rep., 2018.

[4] P. Guan, D. Wu, T. Tian, J. Zhou, X. Zhang, L. Gu, A. Benjebbour, M. Iwabuchi, and Y. Kishiyama, "5G Field Trials: OFDM-Based Waveforms and Mixed Numerologies," *IEEE Journal on Selected Areas in Communications*, vol. 35, no. 6, pp. 1234–1243, June 2017.

[5] D. Kurita, K. Tateishi, A. Harada, Y. Kishiyama, S. Parkvall, E. Dahlman, and J. Furuskog, "Field Experiments on 5G Radio Access Using Multi-Point Transmission," in *Proc. 2015 IEEE Globecom Workshops*, Dec 2015, pp. 1–6.

[6] Telecommunication Standardization Sector of ITU, "Y.3101 - Requirements of the IMT-2020 network," ITU-T, Tech. Rep., 2018.

[7] 5G PPP Architecture Working Group, "View on 5G Architecture," 5G PPP, Tech. Rep., 2017.

[8] *5G Network Architecture and Design*. Accessed on 20th February 2019. [Online]. Available: https://es.slideshare.net/3G4GLtd/5g-network-architecture-and-design

[9] J. Navio-Marco, J. Riol-Martín, and R. Pérez-Leal, "Towards 5G: Techno-economic analysis of suitable use cases," *NETNOMICS: Economic Research and Electronic Networking*, September 2018.

[10] M. Rupp, S. Schwarz, and M. Taranetz, *The Vienna LTE-Advanced Simulators: Up and Downlink, Link and System Level Simulation*, 1st ed., ser. Signals and Communication Technology. Springer Singapore, 2016.

[11] T. S. Rappaport, *Wireless Communications: Principles and Practice*, 2nd ed. Prentice Hall, 2002.

[12] *Propagation data and prediction methods for the planning of short-range outdoor radiocommunication systems and radio local area networks in the frequency range 300 MHz to 100 GHz*, ITU Std. Recommendation ITU-R P.1411-9, 2017.

[13] *Study on 3D channel model for LTE*, 3GPP Std. TR 36.873 V12.0.0 Release 12, 2014.

[14] ITU-R, "Guidelines for evaluation of radio interface technologies for IMT-2020," ITU, Tech. Rep., 2017.

[15] *Study on channel model for frequencies from 0.5 to 100 GHz*, 3GPP Std. TR 38.902 V14.3.0 Release 14, 2018.

[16] Y.-W. Kuo and L.-D. Chou, "Power Saving Scheduling Scheme for Internet of Things over LTE/LTE-Advanced Networks," *Mobile Information Systems*, vol. 2015, pp. 1–11, 12 2015.